Biochimica et Biophysica Acta 862 (1986) 134–140
Elsevier

BBA 73325

Atomic and Raman spectroscopy of the dipalmitoylphosphatidic acid-calcium complex and phase transitions

Ellen Bicknell-Brown [a], Kenneth G. Brown [b] and Douglas Borchman [a]

[a] *Department of Chemistry, Wayne State University, Detroit, MI and*
[b] *Department of Chemical Sciences, Old Dominion University, Norfolk, VA (U.S.A.)*

(Received 23 June 1986)

Key words: Phosphatidic acid; Calcium binding; Lipid bilayer; Raman spectroscopy; Liposome; Phase transition

Calcium binding measurements by atomic absorption spectroscopy and temperature-dependent phase transitions studies by Raman spectroscopy were combined in order to investigate the effect of Ca^{2+} binding on dipalmitoylphosphatidic acid (DPPA) dispersed in $CaCl_2$ solutions of varying concentration at pH 7. The peak heights for the Raman CH stretch bands observed at 2885 cm^{-1} and 2935 cm^{-1} were used as a measure of hydrocarbon chain randomization and aggregate ultrastructure. Two transitions were observed for both pure DPPA and DPPA-Ca^{2+} mixtures. Ca^{2+} binding caused greatly increased DPPA chain rigidity in the melted state above T_m, but had much less effect on the solid phases below T_m. The increase in rigidity in the fluid state was observed to vary linearly with the molar ratio of bound Ca^{2+} to total DPPA throughout the range 0 to 1. The results of the Raman and Ca^{2+} binding measurements are explained by a model in which two populations of DPPA co-exist in the fluid state when Ca^{2+} binding has not reached saturation. One population consists of the Ca^{2+}-bound DPPA complex with stoichiometric 1:1 binding ratio (determined from an atomic absorption Ca^{2+} binding study), and the second population is free DPPA. We propose that Ca^{2+}-induced clustering and separation of the two components occurs chiefly because of differences in chain fluidity of the two components.

Introduction

The binding of calcium to phosphatidic acid is of considerable interest, since binding of divalent cations to acidic lipids has been implicated in the processes of lateral phase separation in mixed lipid systems [1] and vesicle fusion [2,3]. It has also been suggested that increased phosphatidic acid turnover is linked to sealing of neurotransmitter vesicles and to external calcium ion concentration [4].

Although the geometry and molar ratio of the binding of calcium ion to phosphatidic acid has been a matter of speculation, the high stability of the calcium-phosphatidic acid complex is well documented. The affinity of phosphatidic acid for Ca^{2+} is much greater than that for sodium, lithium, potassium [5] and hydrogen ions [6]. The stability constant for phosphatidic acid-calcium binding has been measured by various techniques. Values obtained vary somewhat, but are generally above 10^4 M^{-1} [5]. Measurements are made difficult because the stability constant may be dependent on ionic strength and because multiple equilibria, involving hydrogen ion binding and calcium-phosphatidic acid binding complexes, may be present.

Calcium ion has been observed to affect the phase of phosphatidic acid in aqueous dispersion.

Abbreviation: DPPA, dipalmitoylphosphatidic acid.

Correspondence: Dr. K.G. Brown, Department of Chemical Sciences, Old Dominion University, Norfolk, VA 23508, U.S.A.

Langmuir trough experiments [7] have shown that Ca^{2+} causes condensation of phosphatidic acid. Other studies have shown that divalent cations shift the pH, and consequently the transition temperature, of phosphatidic acid dispersions by displacing hydrogen ion [8].

The present study utilizes Raman spectroscopy as a non-perturbative probe of bilayer phase transitions to study the Ca^{2+}-phosphatidic acid complex and its affect on bilayer phases at constant pH 7. In order to obtain more information about the affect of Ca^{2+} on phosphatidic acid phases, we have combined atomic spectroscopy studies, which we use to measure the degree of calcium saturation of the DPPA, with Raman spectroscopy studies, which are used to monitor bilayer packing and phase transitions.

Materials and Methods

Dipalmitoylphosphatidic acid (Sigma, 99%) was measured for purity by silica gel thin layer chromatography. The chromatogram showed a characteristic single band. Calcium was not detectable in the sample by atomic absorption nor by atomic emission spectroscopy. 1.91 mol Na^+ per mol DPPA was measured by emission spectroscopy. Most of that Na^+ was removed by dialysis.

Each Raman sample was prepared by first dispersing 4 mg DPPA in 1.00 ml triply distilled deionized water. Weights of DPPA and H_2O were measured to 0.1 mg accuracy with a Cahn electrobalance. The dispersion was adjusted to pH 7.0 and allowed to incubate 4 h at 80°C. 10–60 μl volumes of 0.5 M $CaCl_2$ were added by calibrated pipettes. The concentration of the 0.5 M $CaCl_2$ solution used was determined to three decimal places by emission spectroscopy. The sample was stirred by magnetic stirrer at 80°C for 2 h and pH was again adjusted to 7.0. The sample was then stirred at room temperature for 24 h and, if required, the pH was again adjusted to 7.0. The DPPA sample was compacted by a table-top centrifuge and then placed in a capillary tube and sealed for Raman measurement. An aliquot of the excess supernatant was analysed by Ca^{2+} emission spectroscopy to determine the amount of Ca^{2+} removed from the aqueous phase by DPPA.

Raman samples in sealed capillary tubes were measured in a Harney Miller cell which regulated sample temperature by a stream of warmed or cooled N_2 gas. A thermocouple was attached to the sample capillary close to the site at which the laser beam was incident. Temperature fluctuation during each Raman measurement was less than 1.0°C. 45 min equilibration time was allowed between each temperature increment and the Raman measurement. The 514.5 nm laser line of an argon ion laser was used for sample excitation. Scattered light was collected at 90°C to the incident beam and analyzed by a Spex 14018 double monochrometer equipped with a spatial filter to reduce stray light. The photon counting system includes a cooled RCA-C31034 photomultiplier tube. Spectral bandpass was set at 5 cm^{-1}.

Data for the phosphatidic acid-calcium ion binding curve were obtained by emission spectroscopy. Samples were prepared in the manner described above for Raman samples. Aliquots of supernatant were removed and analyzed for Ca^{2+} by emission spectroscopy. Phosphate analysis indicated no measurable amount of lipid was present in the supernatants. The number of moles bound Ca^{2+} was determined as the difference in number of moles Ca^{2+} in solution before and after incubation with DPPA.

Results

To gain information about the stoichiometry of the DPPA-Ca^{2+} binding at saturation, a binding curve was obtained by analyzing by atomic emission spectroscopy the amount of free Ca^{2+} in solution in the supernatant of DPPA-Ca^{2+} mixtures. The molar ratio of bound Ca^{2+} to total DPPA is plotted against free Ca^{2+} concentration in the bulk solution in Fig. 1. From the binding curve, we observe saturation occurs with a one-to-one stoichiometric binding ratio for the Ca^{2+}-DPPA complex. As a rough estimate for the binding constant, we assumed a single value over the range of Ca^{2+} concentrations studied and obtained the value $2.4 \cdot 10^4$ M^{-1}, which agrees closely with values measured previously [5]. However, it was clear from our data that the apparent binding constant decreases slightly with increasing Ca^{2+} ionic strength.

Temperature dependence of the Raman C-H

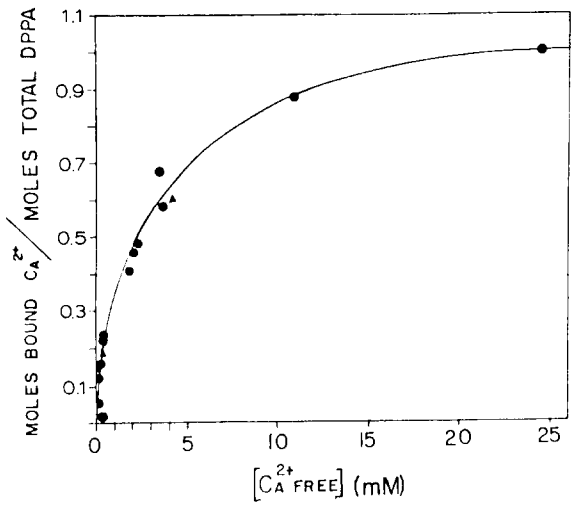

Fig. 1. Calcium-binding curve for DPPA. Circles indicate data measured by atomic spectroscopy. Triangles indicate supplemental data obtained by EDTA titration.

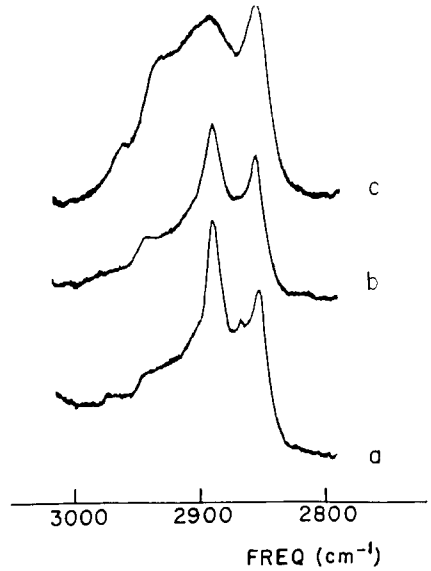

Fig. 2. Raman CH stretch region for an aqueous dispersion of DPPA at (a) 10, (b) 22, and (c) 75°C.

stretch region for DPPA dispersed in water is illustrated in Fig. 2 for three temperatures; 10, 22 and 75°C. The relative intensity of the Raman Fermi resonance enhanced antisymmetric CH_2 stretch mode observed at 2885 cm^{-1} decreases as the hydrocarbon chains are randomized by increasing temperature [9].

The intensity ratio of the antisymmetric 2885 cm^{-1} and symmetric 2845 cm^{-1} CH_2 stretch modes is a sensitive marker for lipid phase packing. In a Raman temperature study of dipalmitoylphosphatidylcholine, we have observed, with I_{2885}/I_{2845} ratios, three transitions between 0 and 50°C. The ratio changes from 1.60 to 1.44 at 4°C, from 1.44 to 1.33 at 17°C (subtransition), from 1.33 to 1.25 at 32°C (pretransition), and from 1.25 to 1.0 at 41°C (main transition). The intensity ratio, I_{2885}/I_{2845}, for DPPA at 10°C (Fig. 2a) is 1.42. This is approximately the value of 1.44 for DPPC below the 17°C subtransition, and is assigned to a "crystal-like" phase. I_{2885}/I_{2845} for DPPA at 22°C (Fig. 2b) is 1.2 and is therefore approximately that of DPPC above the pretransition, a phase described as hexagonal and 'ripple-like'. The determining factors for the intensity distribution in the C-H stretching region, under the experimental conditions of this study, are the extent of hydrocarbon chain order and the interchain interaction [10]. The chain order is equivalent for these two molecules, at this value of the C-H ratio, since the C-C stretching region of the spectra yields identical *gauche-trans* ratios. The packing of the chains must, then, be similar. Therefore, we assign the phase of DPPA at 22°C to a 'ripple-like' phase with hexagonal packing.

The relative intensity of the 2935 cm^{-1} asymmetric CH_3 stretch mode increases with chain randomization [11]. By plotting the peak height ratio of the 2935 and 2885 cm^{-1} bands we accentuate the phase changes for the hydrocarbon chains. The intensity ratio I_{2935}/I_{2885} is plotted against temperature in Fig. 3 for samples of DPPA with varying degrees of Ca^{2+} binding.

Fig. 3a represents the temperature-induced hydrocarbon chain randomization for DPPA with no Ca^{2+} present. Two transitions appear in the diagram, a small transition at 18°C and the main transition at about 60°C. We refer to the temperatures of these transitions as T_p and T_c, respectively.

The transition at T_p probably consists of a packing change, perhaps similar to the pre-transition observed in DPPC [12,13]. A band at about 2865 cm^{-1}, which is most likely due to the CH_3 symmetric stretch, is present in the spectrum of DPPA below T_p (Fig. 2a); but is absent above T_p (Fig. 2b). A similar 2865 cm^{-1} band was observed below, but not above, the pre-transition for DPPC

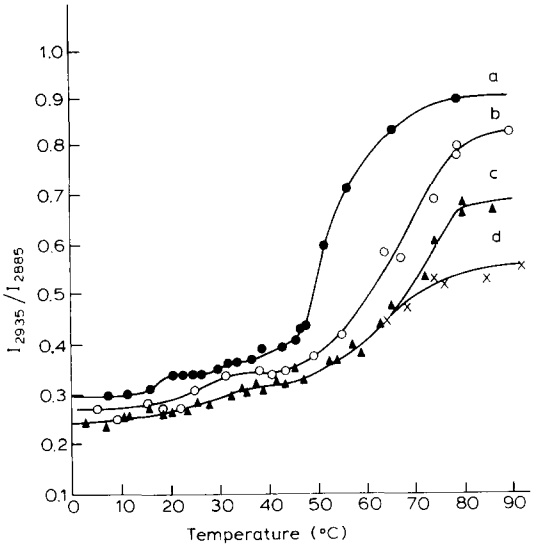

Fig. 3. Temperature dependence of I_{2935}/I_{2885} for aqueous dispersions of DPPA with bound Ca^{2+} for DPPA molar ratios of (a) 0, (b) 0.18, (c) 0.60 and (d) 1.0. The data points below 60°C, in the equimolar mixture, exhibit the same behavior as that seen for the 0.60 molar ratio. The S.D. for each point is ±0.02.

[13]. However, as discussed above, the I_{2885}/I_{2845} intensity ratios suggest that DPPA transition involves a change from a more crystal-like phase to the hexagonal phase. This may explain the large temperature difference between the two DPPA transitions.

Effect of Ca^{2+} binding on transition temperature

The molar ratios of bound Ca^{2+} to total DPPA at pH 7.0 measured for the Raman samples are 0 (Fig. 3a), 0.18 (Fig. 3b), 0.60 (Fig. 3c) and 1.0 (Fig. 3d). The total Ca^{2+} concentrations (bound and free) are 0, 1.5, 6, and 200 mM, respectively. We observe (Fig. 3) that bound Ca^{2+} increases both T_p, the packing transition temperature, and T_c, the hydrocarbon chain melting temperature. A broad post-melting region is observed above T_c in DPPA with no Ca^{2+} present. Some asymmetry in the melting curve for DPPA has also been observed by DSC [14]. The broad post-melting region is not apparent with addition of Ca^{2+}. However, symmetric broadening of the transition and loss of cooperativity is evident from the Raman melting curves for DPPA with Ca^{2+} binding.

The phase transition curves show that Ca^{2+}

TABLE I

TRANSITION PROPERTIES FOR DPPA DISPERSIONS WITH VARYING DEGREES OF Ca^{2+} BINDING SATURATION

Total Ca^{2+} (mmol/l)	Free bulk $[Ca^{2+}]$ (nM)	mol bound Ca^{2+} per mol total DPPA	T_p (°C)	T_c (°C)
0	0	0	18	57
1.5	0.47	0.18	26	66
6.0	4.09	0.60	30	69

causes the temperatures T_p and T_c to shift by 6–12 Cdeg at pH 7. Approximate midpoint temperatures for T_p and T_c were determined from van't Hoff plots of ln K vs. $1/T$, where values for ordered and disordered population ratio were estimated from the I_{2935}/I_{2885} intensity ratios. The results are presented in Table I. With the binding of 0.18 calcium ions per DPPA molecule, T_p increases from 18 to 26°C and T_c increases from 57 to 66°C. With the binding of 0.60 Ca^{2+}/DPPA, T_p increases to 30°C and T_c increases to 69°C. We note that (1) the increase in T_p and T_c with increased Ca^{2+} binding falls off as the Ca^{2+} binding increases, and (2) that the temperature interval between T_p and T_c remains fairly constant at about 40°C. These results suggest that the dominant mechanisms in both transitions are probably very similar and probably involve headgroup interactions.

Effect of Ca^{2+}-binding on structure above T_c

The relative change in the peak height ratio I_{2935}/I_{2885} provides a measure of the extent of hydrocarbon chain ordering which occurs as a function of the degree of Ca^{2+} binding. The peak height ratios I_{2935}/I_{2885} are slightly depressed by Ca^{2+} at temperatures, below the main transition, indicating some ordering of the gel state at temperatures both below T_p and between T_p and T_m. The ordering affect of Ca^{2+} is most evident above T_c. Each increase in the molar ratio of bound Ca^{2+} to DPPA further depresses the value of I_{2935}/I_{2885} above T_c. Increased Ca^{2+} binding continues to broaden the main transition and to reduce the extent of chain disordering melting at the

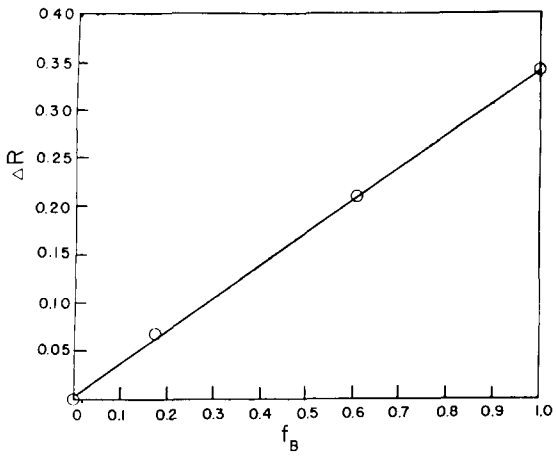

Fig. 4. The change in the ratio I_{2935}/I_{2885} above T_c as a function of the fraction DPPA bound to Ca^{2+}.

transition throughout the entire range of bound Ca^{2+}/total DPPA. We observe a broadened, reduced transition around 70°C, even for Ca^{2+}-saturated DPPA, although this transition was not observed by DSC for Ca^{2+}-DPPA mixtures of molar ratio greater than 0.3 [15]. Apparently, this is because the Raman technique is also sensitive to conformational changes which may lack a high degree of cooperativity.

The depression of I_{2935}/I_{2885} for the disordered state above T_c is proportional to the fraction DPPA bound to Ca^{2+}. This is clearly demonstrated in Fig. 4, where the Ca^{2+} induced intensity ratio change ($R_0 - R$) is plotted against mol Ca^{2+} bound per mol DPPA (f_b). The four values of $R_0 - R$ are co-linear, showing that

$$R_0 - R = f_b(R_0 - R_{1.0})$$

where:

$R = I_{2935}/I_{2885}$ for the state above T_c

$R_0 = R$ for the case with no Ca^{2+} bound,

$R_{1.0} = R$ for the case with 1.0 mol Ca^{2+} bound per DPPA.

The change in extent of bilayer ordering is therefore proportional to the molar ratio of bound Ca^{2+} to total DPPA. This result indicates that at pH 7 the stoichiometry of the major calcium ion phosphatidic acid complex is 1 : 1 at all fractions of Ca^{2+} binding saturation above 0.18 and, therefore, that the fraction of DPPA population bound is equal to the molar ratio bound Ca^{2+}-to-DPPA, f_b. The combined Raman and atomic emission spectroscopy results are best interpreted by assuming a binary structure in which a population of free phosphatidic acid and a population of the 1 : 1 Ca^{2+}-phosphatidic acid complex co-exist.

Conclusion

Binding ratio of the Ca^{2+}-phosphatidic acid complex

The binding of Ca^{2+} to phosphatidic acid has been frequently compared to Ca^{2+}-phosphatidylserine binding, and it has been suggested that phosphatic acid molecules may also be bridged by Ca^{+2} in a 2 : 1 molar ratio bound phosphatidic acid to bound Ca^{2+} at physiological concentrations [7]. The molar ratio of phosphatidylserine (PS) to bound Ca^{2+} has been observed to increase to 2 at 1 mM Ca^{2+} concentration [16,17], whereupon extensive bilayer reorganization is reported to take place [15]. Surface radioactivity measurements yielded an absorption isotherm indicating the ratio of PS/Ca^{2+} in the complex is 2 at Ca^{2+} concentrations below 0.1 mM and approaches 1 at Ca^{2+} concentration of 1 mM. For DPPA, the results of the binding curve (Fig. 1) indicate that the Ca^{2+}-DPPA binding ratio is 1 : 1 at saturation, in agreement with earlier observations by calorimetry and small angle x-ray scattering [19]. The linear dependence of Ca^{2+} hydrocarbon chain ordering above T_c (evidenced by the intensity ratio I_{2935}/I_{2885}) demonstrates that DPPA and Ca^{2+} form a complex with a 1 : 1 stoichiometric ratio at pH 7.0, even when Ca^{2+} binding is as low as 0.18 of saturation. It is likely that the net charge of the complex is zero, since Ca^{2+} is able to replace hydrogen ion on the phosphate group, requiring readjustment of the pH.

The effect of temperature upon the binding of Ca^{2+} is expected to be minimal, because the interaction is expected to be electrostatic, which, based upon the Gouy-Chapman theory, is not strongly temperature-dependent [22] over the relatively narrow temperature range studied.

Clustering of the Ca^{2+}-DPPA complex in the liquid-crystalline phase

A phase transition with a low degree of cooper-

ativity is observed at saturation of the bilayer with Ca^{2+}, although the calorimetric data of Liao and Prestegard [19] seem to indicate non-cooperative behavior without a definite phase transition when saturation occurs. A cooperative phase transition with a broadened post-melting region is observed for DPPA with no Ca^{2+} present. The kinetics of the gel–liquid-crystal phase transition have been measured for phosphatidic acid using an ion-jump technique in which Ca^{2+} or H^+ was used to make the bilayer more solid [20]. The mechanism for rigidifying the bilayer was determined to be nucleation with a half-life of the order 10 to 100 ms. The usual kinetics of mechanisms involved in the main transition of phospholipids are much slower than the lifetime of the Raman effect (10^{-13} to 10^{-15} s). Therefore, both states in a mixed state system with $0 < f_b < 1$ are observed, rather than an average for the two states. We might expect to observe two main transitions, one for free DPPA and one for Ca^{2+}-bound DPPA. In the samples studied, it appears that broadening and loss of cooperativity obscure the relatively small Ca^{2+}-induced difference in the transition temperature of the bound and free DPPA populations, so that two separate transitions are not observed in the melting curves for samples with $f_b = 0.18$ and 0.60.

The broadened post-melting region above T_c, where the I_{2935}/I_{2885} ratio continues to increase slowly by a relatively small amount, gives an asymmetric shape to the melting curve produced at T_c by the Raman intensity ratios. In the post-melting region the intensity ratio increases to values corresponding to those observed for melted liposome bilayers. Therefore, it appears that upon melting, DPPA at pH 7 retains a liposome structure. Binding of Ca^{2+} at pH 7 appears to stabilize the bilayers of the larger aggregates (liposomes) by rigidifying the hydrocarbon chains. In contrast, addition of Ca^{2+} to unsaturated phosphatidic acid at pH values below 5 helps promote formation of inverted micelles (or intermediate structures), which are also induced at low pH without addition of Ca^{2+} [7]. Miner and Prestegard [21] have also demonstrated the presence of hexagonal II phases above T_c for Ca^{2+}-phosphatidic acid complexes of shorter-chain saturated (C_{12}) and longer-chain unsaturated phosphatidic acids. Therefore, the nature of the effect of Ca^{2+} on the aggregate structure depends on pH and/or chain saturation.

These two observations – (1) Ca^{2+} stabilizes a rigid lamellar ultrastructure above T_c and (2) the chain ordering is linearly proportional to the molar ratio bound Ca^{2+} to DPPA – suggest that lateral separation of DPPA into a Ca^{2+}-bound DPPA population and a Ca^{2+}-free DPPA population exists above T_c.

The Ca^{2+} induced clustering of DPPA into separate domains above T_c does not occur by Ca^{2+} bridging, because the binding stoichiometry ratio is 1 : 1, even for 0.18 saturation. Nor is it driven directly by electrostatic forces, because the repulsive forces of interacting free phosphatidate ions would be mitigated by intervening Ca^{2+}-DPPA complexes. Because the bound Ca^{2+} greatly reduces the fluidity of DPPA in the liquid-crystal state above T_c, we propose that the Ca^{2+}-DPPA complex and free DPPA are separated because of the large difference in rigidity of the hydrocarbon chains for the two populations. Thus, favorable hydrocarbon chain interactions are achieved for the Ca^{2+}-DPPA complex above T_c by clustering of the neutral Ca^{2+}-DPPA complex. Increased favorable interactions between bilayers may also occur at the sites of clustering.

References

1 Fraley, R., Wilschut, J., Duzgunes, N., Smith, C. and Papahadjopoulos, D. (1980) Biochemistry 19, 6021–6029

2 Wilschut, J., Duzgunes, H., Fraley, R. and Papahadjopoulos, D. (1980) Biochem. 19, 6011–6021

3 Papahadjopoulos, D., Poste, G., Schaeffer, B. and Vail, W. (1974) Biochim. Biophys. Acta 352, 10–28

4 Hawthorne, J.M. (1976) Structure of Biological Membranes (Abrahamsson, S. and Pascher, I., eds), pp. 235–244, Plenum Press, New York

5 Abramson, M.B., Katzman, R., Gregor, H. and Curci, R. (1966) Biochemistry 5, 2207–2213

6 Abramson, M.B., Katzman, R. and Gregor, H.P. (1964) J. Biol. Chem. 239, 70–76

7 Papahadjopoulos, D. (1968) Biochim. Biophys. Acta 163, 240–254

8 a) Trauble, HH. and Eibl, H. (1974) Proc. Natl. Acad. Sci. USA 71, 214
b) Trauble, H. (1977) Structure of Biological Membranes, Nobel Foundation Symposium 34, (Abrahamson, S. and Pascher, I., eds.), pp. 509–550, Plenum Press, New York

9 Brown, K.G., Peticolas, W.L. and Brown, E.B. (1973) Biochem. Biophys. Res. Commun. 54, 358–356

10 Snyder, R.G., Strauss, H.L. and Elliger, C.A. (1982) J. Phys. Chem. 86, 5145–5150
11 Hill, I.R. and Levin, I. (1979) J. Chem. Phys. 70, 842–847
12 Gaber, B.P., Yager, P. and Peticolas, W.L. (1977), Biochim. Biophys. Acta 465, 260–268
13 Gaber, B.P., Yager, P. and Peticolas, W.L. (1978) Biophys. J. 21, 161–170
14 Papahadjopoulos, D. and Bangham, A.D. (1966) Biochim. Biophys. Acta 126, 185–188
15 Papahadjopoulos, D., Vail, W.J., Jacobson, K. and Poste, G. (1975) Biochim. Biophys. Acta 394, 483–491
16 Newton, C., Pangborn, W., Nir, S. and Papahadjopoulos, D. (1978) Biochim. Biophys. Acta 506, 281–287
17 Hauser, H., Drake, A. and Phillips, M.C. (1976) Eur. J. Biochem. 62, 335–344
18 Lansman, J. and Haynes, D.H. (1975) Biochim. Biophys. Acta 394, 335–347
19 Liao, M.J. and Prestegard, J.H. (1981) Biochim. Biophys. Acta 645, 149–156
20 Strehlow, U. and Jahnig, F. (1981) Biochim. Biophys. Acta 641, 301–310
21 Miner, V.W. and Prestegard, J.H. (1984) Biochim. Biophys. Acta 774, 227–236
22 Starzak, M. (1984) The Physical Chemistry of Membranes pp. 178–184, Academic Press, New York